

On the Stability of Metallic Pt-Ni Foams during Oxidative Steam Reforming of Fuel Grade Ethanol

Concetta Ruocco*, Vincenzo Palma, Antonio Coppola

University of Salerno, Department of Industrial Engineering, Via Giovanni Paolo II 132, 84084 Fisciano (SA), Italy
ruocco@unisa.it

In this work, bimetallic catalysts (Pt-Ni/CeO₂-Al₂O₃) in the form of powder and structured samples were employed for the oxidative steam reforming of fuel grade bioethanol. The stability performance of the above samples was investigated in a stainless steel tubular reactor at 500°C and 1 atm by feeding a commercial fuel grade ethanol stream with a H₂O/C₂H₅OH = 4 and O₂/C₂H₅OH = 0.5. Preliminarily, the ceria loading (between 25 and 45 wt%) as well as the Pt content (between 2 and 5 wt%) were optimized with respect to the washcoat (wc) content for the powder sample. Stability tests were carried out for 24 hours at 500°C and WHSV (Weight Hourly Space Velocity) = 12 h⁻¹. The highest endurance performance was recorded over the 3Pt-10Ni/35CeO₂/wc, which assured an ethanol conversion of almost 98% at the end of the test with a corresponding hydrogen yield of 50%. When the most promising formulation was transferred on a Ni-Fe substrate (made of an open cell foam), a clear improvement in the catalyst performance was recorded. In particular, the structured catalyst, able to assure a very good heat management within the catalytic bed as well as an improved mass transport, displayed a more stable behaviour compared to the corresponding powder, even in the presence of the typical bioethanol impurities; moreover, no significant formation of unwanted by-products (coke precursors) was observed during 24 hours of time-on-stream (TOS).

1. Introduction

Energy demand growth and the serious concerns about pollution produce a considerable boost towards the use of alternative fuels (i.e. hydrogen). In this regard, the use of renewable sources allows generating almost zero greenhouse gases (Peres A.P.G. et al., 2013). Bioethanol, obtained via the microbial fermentation of biomass wastes, can be directly used for H₂ generation through the reforming process (Mulewa W. et al., 2017). Bioethanol is produced from renewable feedstocks (i.e. cereal crops, sugar cane and lignocellulosic crops); however, in the last few years, heavy concerns related to the use of food crops for fuel purposes have pushed the researchers' interests towards the employment of second generation ethanol. In fact, the latter source is based on non-food raw material, which do not compete against food supplies (Kumar D. et al., 2012).

The main components of crude bioethanol (i.e. bioethanol produced from biomass without downstream purification) are water, ethanol, and a series of impurities such as alcohols (C1, C3, and C4), aldehydes (C3 and C4), acetone, organic acids (acetic acid and lactic acid), amines, glycerol, and esters in different concentrations depending on the bioethanol source (Lazar D.M. et al., 2019, Souza E.L. et al., 2014).

The ethanol steam reforming reaction is expected to involve only CO₂ and H₂ formation (Anil et al., 2022). However, many side pathways may occur, causing reduced yields and carbon deposition. This latter issue appears even more prominent when raw feeds are selected, which may cause a faster coke accumulation. Thus, ethanol reforming in the presence of the typical bioethanol impurities has been rarely investigated in recent literature (Ruocco C. et al., 2022). In this regard, the search for highly active, selective and stable catalysts appears a long-standing topic. In particular, when crude bioethanol is fed to the reformer, higher alcoholic contaminants may improve hydrogen yield (due to the enhanced contribution of reforming pathways). However, the catalyst deactivation rate can also grow, as a consequence of the promoted carbon deposition. Among the previous formulations employed for raw bioethanol reforming, the samples containing rare earth oxides (i.e. CeO₂ or La₂O₃) were shown to improve the gasification rate of eventually deposited carbon species

(both in amorphous and graphitic form) (Cerdà-Moreno C. et al., 2019). Likewise, addition of noble metals such as Pt and Rh to the catalyst lead to reduced carbon formation even in the presence of amines (Bilal M. et al., 2017).

Recently, structured catalysts were shown to increase the durability of the conventional counterparts, due to the overcome heat and mass transfer limitations. However, to the best of our knowledge, structured catalysts have been rarely employed for the oxidative steam reforming of raw bioethanol.

In this work, the effect of the deposition of a bimetallic catalyst formulation on a structured metallic carrier has been investigated for oxidative steam reforming of ethanol (OESR). In order to assure a good adhesion of the catalyst of the metallic foam, the formulation of a previous developed catalyst (Pt-Ni/CeO₂) was properly modified through the addition of Al₂O₃ (Ruocco et al., 2019). In particular, this study was focused on the evaluation of the influence of the CeO₂/Al₂O₃ ratio (ranging from 25 to 45 %) as well as Pt content (in the interval 3-5%) on the catalyst's performance during OESR. Catalyst activity and stability was investigated at 500°C, H₂O/C₂H₅OH=4 and O₂/C₂H₅OH=0.5 and WHSV=12 h⁻¹. The most stable formulation was identified from the above screening and transferred on a structured carrier (Ni-Fe open-cells foam); the effect of the foam structure on the activity and durability of the final catalyst was also investigated.

2. Experimental

The powder catalysts used in this work were synthesized from the calcined washcoat (wc) slurry. For the washcoat preparation, γ -alumina (PURALOX SCCa 150/200, SASOL), was grinded by means of a Retsch RM100 mill to reach a particles size dimension lower than 10 μm . Subsequently, alumina was added to a colloidal solution containing methylcellulose (Sigma-Aldrich) and pseudoboehmite (Pural SB, provided by SASOL). The resulting suspension was acidified at pH= 4 with nitric acid (65%, Carlo Erba Reagenti). Thereafter, the milled alumina was added in the colloidal solution, which was vigorously mixed under mechanical stirring. The final composition of the slurry was: 1 wt% of methylcellulose, 4.6 wt% of pseudoboehmite and 15.4 wt% of γ -alumina. Finally, the slurry was dried overnight and calcined at 600°C for 3 hours. CeO₂, Ni and Pt were sequentially deposited on the calcined washcoat starting from Cerium(III) 2,4-pentanedionate hydrate, nickel nitrate hexahydrate and platinum chloride (provided by Carlo Erba), respectively. Different catalysts were prepared by changing the ceria content in the interval 25-45 wt% (with respect to the washcoat mass) and the Pt loading from 2 to 5 wt% (with respect to the ceria content). Conversely, the Ni content was fixed to 10 wt% with respect to the ceria mass, on the basis of previous studies (Ruocco C. et al., 2019). The catalytic samples were denoted as a Pt-10Ni/bCeO₂/wc, where a and b refer to Pt and CeO₂ content, respectively.

For the preparation of the structured catalyst, the washcoat, ceria and active species deposition were sequentially carried out. Ni-Fe open cell foams, (15-20 ppi, d=2 cm, L=5 cm) provided by VIM technology Ltd, were dipped into the washcoat suspension for 20 min at ambient temperature. Thereafter, centrifugation, drying and calcination occurred; the washcoating procedure was repeated until reaching a final loading of 0.2 g·cm⁻³. Once deposited the washcoat on the carrier, the following steps of ceria, nickel and platinum deposition were carried out as described above for the powder samples.

The fresh and spent catalysts were characterized by surface area measurements (BET analysis), X-ray diffraction analysis (XRD) and Temperature Programmed Reduction (TPR) measurements. In addition, the amount of carbon deposited during OESR reaction was measured via Thermogravimetric analysis.

The catalysts performance during the oxidative steam reforming (OESR) of commercial fuel grade bioethanol was investigated at 500°C under atmospheric pressure in a tubular quartz reactor (i.d.= 2.54 cm). The powder catalyst (typically 1.5 g), crushed and sieved to reach a particle size distribution of 180-355 μm , was diluted with quartz particles (500-710 μm) in a volumetric ratio of 1:1, sandwiched between two quartz wool flakes and loaded into the reactor. For the structured catalysts tests, the foam was simply wrapped into the quartz wool. After catalyst reduction in situ, the feeding stream (bioethanol, water and diluting argon) was sent to a boiler for vaporization (T=170°C); oxygen can be mixed with the reacting stream directly in correspondence to the reactor inlet. The feeding composition can be monitored online by means of a mass spectrometer provided by Hiden Analytical; meanwhile, it is possible to wash the reactor with a stream of nitrogen. A system of 4 two-way valves, placed into a heated block, allows to switch from the by-pass to reactor configuration. The final composition of the reacting stream was: 10% bioethanol, 40% H₂O, 5%O₂ and 45% Ar. The weight hourly space velocity (WHSV), defined as the ethanol mass flow-rate normalized with respect to the catalytic mass, was fixed at 12 h⁻¹. The corresponding contact time (80 ms) was very low and was chosen to study the catalytic behavior under stressing conditions. The results of the stability tests were compared in terms of ethanol conversion (X), H₂ yield (Y_{H₂}) and C-containing products yield (Y_i), as previously defined (Ruocco C. et al., 2019).

After stability tests, the amount of carbon eventually deposited on the spent catalysts was evaluated through temperature programmed oxidation measurements (TPO), performed by heating the sample from ambient temperature to 1000°C under a 5%O₂ in Ar stream. The resulting carbon formation rate (CFR) was calculated

by normalizing the carbon mass with respect to the catalytic mass, the hours of test and the amount of carbon fed as ethanol.

3. Results & Discussion

3.1 Results of the fresh catalysts characterization

The results of BET, XRD and TPR analysis were synthesized in Table 1. Due to the increase of ceria content, a slight reduction of the specific surface areas of the samples was recorded, with a consequent growth of the ceria particles sizes. Conversely, by changing the Pt loading from 2 to 5 wt%, an improvement in terms of both surface area and ceria particles dispersion was achieved.

Table 1: BET, XRD and TPR values recorded for the powder catalysts.

Sample	BET ($\text{m}^2\cdot\text{g}^{-1}$)	d_{CeO_2} (nm)	H ₂ uptake (Theoretical)	H ₂ uptake (Experimental)
2Pt-10Ni/25CeO ₂ /wc	114	6.1	1909	3693
2Pt-10Ni/35CeO ₂ /wc	113	6.7	1909	8001
2Pt-10Ni/45CeO ₂ /wc	103	8.2	1909	10183
3Pt-10Ni/35CeO ₂ /wc	125	4.9	2011	9747
5Pt-10Ni/35CeO ₂ /wc	123	5.1	2234	9944

The TPR profiles recorded over the catalysts were compared in Figure 1 while the experimental H₂ uptake were found in Table 1 in comparison with the theoretical values (based on the nominal loadings of the metals).

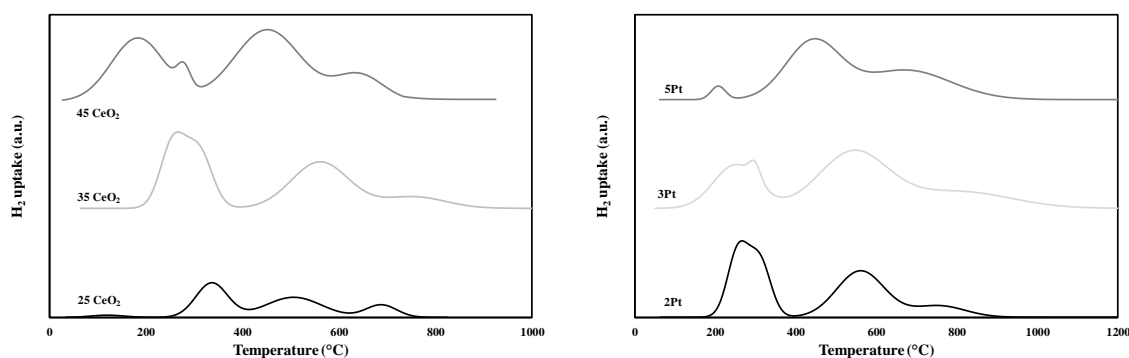


Figure 1: H₂ uptake profiles recorded over the catalysts prepared with different ceria as well as Pt contents.

According to the literature, the reduction peaks observed at low temperature can be linked to the noble metal oxides reduction while the high temperature peaks are ascribed to the nickel phase (Palma et al., 2017). As the ceria particles are very low for all the samples (5-8 nm), hydrogen spillover phenomena were enhanced and the experimental uptakes were considerably higher than the expected values. In particular, the influence of ceria content on the total hydrogen uptake was more pronounced than the effect of platinum loading, with the highest H₂ consumption recorded over the 45%CeO₂-sample and 5%Pt catalyst (Fang B. et al., 2022).

3.2 Results of stability tests: effect of the catalytic formulation

The oxidative ethanol reforming performance of the catalysts containing different CeO₂ and Pt loadings was preliminarily compared in terms of ethanol conversion, as shown in Figure 2.

The growth in the ceria content from 25 to 35 wt% (with respect to the washcoat mass) assured a visible improvement in terms of ethanol conversion; however, a further improvement had a negative impact on catalyst stability, probably due to the CeO₂ dispersion worsening (Table 1). Once fixed the ceria loading to 35 wt%, when platinum content was changed from 2 to 3 wt%, an almost complete ethanol conversion was achieved for 24 hours. In particular, the 5wt% loaded catalyst displayed a worse behavior, with a not negligible by-products formation (not shown).

TPO measurements were performed after stability tests and allowed calculating the carbon formation rate over the spent catalysts. The CFR values have been summarized in Table 2 while Figure 3 shows the CO₂ profiles recorded during carbon oxidation.

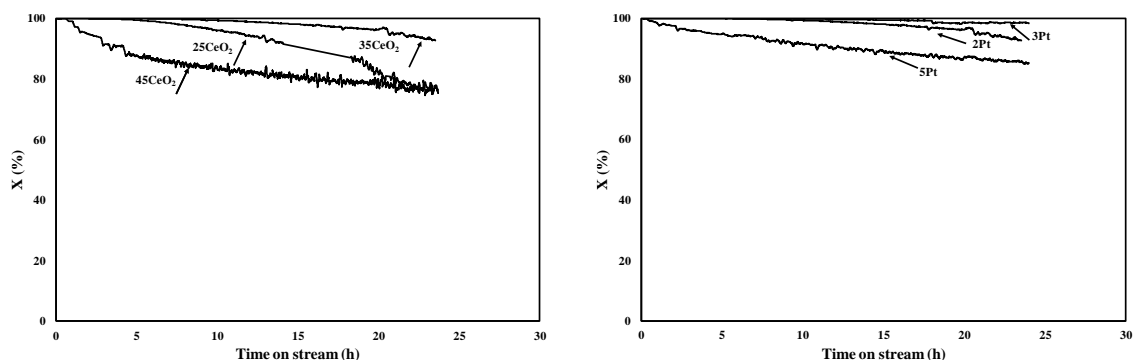


Figure 2. Time-on-stream tests performed over the powder catalysts with different ceria and Pt contents; $T=500^{\circ}\text{C}$, $\text{H}_2\text{O}/\text{C}_2\text{H}_5\text{OH}=4$, $\text{O}_2/\text{C}_2\text{H}_5\text{OH}=0.5$, $\text{WHSV}=12\text{ h}^{-1}$.

Table 2: Results of spent catalysts characterization.

Sample	CFR ($\text{g}_{\text{coke}} \cdot \text{g}_{\text{cat}}^{-1} \cdot \text{h}^{-1} \cdot \text{g}_{\text{carbon, fed}}$)
2Pt-10Ni/25CeO ₂ /wc	$2.6 \cdot 10^{-4}$
2Pt-10Ni/35CeO ₂ /wc	$2.1 \cdot 10^{-4}$
2Pt-10Ni/45CeO ₂ /wc	$3.6 \cdot 10^{-4}$
3Pt-10Ni/35CeO ₂ /wc	$1.1 \cdot 10^{-4}$
5Pt-10Ni/35CeO ₂ /wc	$1.5 \cdot 10^{-4}$

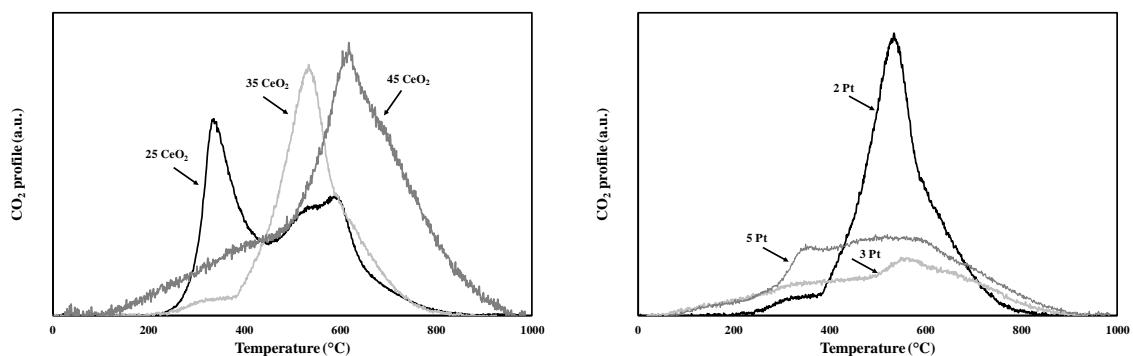


Figure 3. CO₂ profiles recorded during TPO measurements over the spent catalysts.

The increase of ceria loading from 25 to 45% caused a growth in carbon deposition rate, probably due to the dispersion worsening discussed in Par. 3.1. By changing the Pt content from 2 to 3 wt%, an improvement of catalyst resistance towards deactivation was observed. However, a further growth in the Pt loading did not assure the desired gain in terms of catalyst durability. From the CO₂ profiles observed in Figure 3, it is clear that both amorphous and graphitic carbon was deposited over the powder catalysts (Xu T. et al., 2021). In particular, the oxidation of the carbon deposits mainly occurs between 400 and 800°C: the CO₂ formation observed below 550°C is attributed to amorphous coke while the oxidation at 500-800°C can be ascribed to filamentous coke at different carbonization degrees (Guo W. et al., 2022). Despite the contributions of the two peaks is different depending on the selected sample, the total amount of deposited carbon is very low over the 3Pt-10Ni/35CeO₂ sample ($1.1 \cdot 10^{-4} \text{ g}_{\text{coke}} \cdot \text{g}_{\text{cat}}^{-1} \cdot \text{h}^{-1} \cdot \text{g}_{\text{carbon, fed}}$). Conversely, when the ceria loading was increased to 45%, a CFR value almost 3 times higher was recorded.

Based on the above results, the 3Pt-10Ni/35CeO₂-Al₂O₃ was identified as the most stable formulation, which was consequently deposited over the structured metallic foam carrier.

3.3 Results of stability tests: effect of the catalyst structure

The time-on-stream results recorded over the powder catalyst (shown in Figure 1) were compared with the performance obtained by properly depositing the same formulation over the foam catalyst. Figure 4 shows a comparison of the ethanol conversion as well as hydrogen yield profiles recorded in the two cases.

The superior performance of the foam structured catalyst was clearly visible in terms of both ethanol conversion and hydrogen yield profile. In particular, a very stable behavior was recorded: complete conversion was assured and the mean hydrogen yield was above 50%.

Table 3 shows the mean yields towards carbonaceous species measured at the beginning (the first 2 hours) and at the end (the last 1 hours) of the stability tests of Figure 4. In both the cases, acetaldehyde, acetone and ethylene formation was inhibited at the beginning of the test; moreover, the initial products gas distribution was very close to the thermodynamic predictions (calculated through the software Gaseq).

The concentration of C_2H_4 , C_2H_4O and C_3H_6O was still negligible at the end of the test over the structured foam catalyst. Conversely, by-products formation was significant after 24 h of tests in the presence of the powder, which reached an ethylene concentration of 1.3% at the end of the test. The very promising performance observed in the presence of the catalyst deposited on the Ni-Fe foam is ascribable to the support structure. In fact, the use of a thermal conductive structured support with high porosity for the Pt-Ni/CeO₂-Al₂O₃ catalysts allows to improve the thermal exchange inside the reactor.

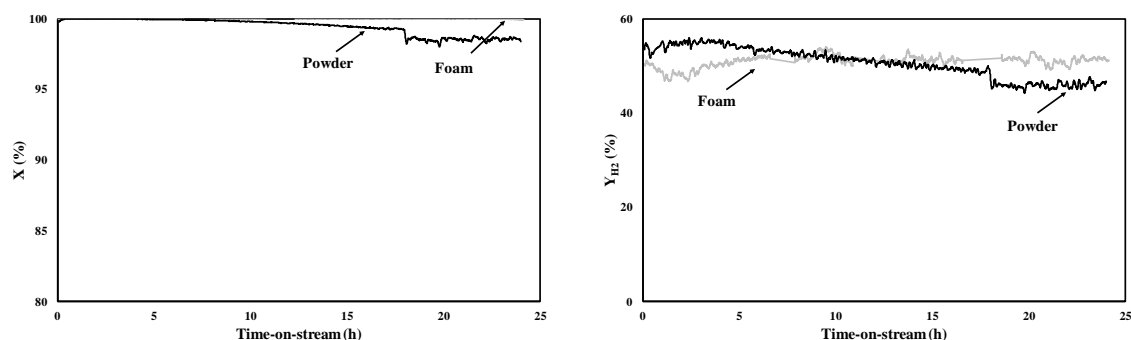


Figure 4. Time-on-stream tests performed over the powder and structured catalysts; $T=500^{\circ}C$, $H_2O/C_2H_5OH=4$, $O_2/C_2H_5OH=0.5$, $WHSV=12\ h^{-1}$.

Table 3: Reaction products yield recorded at the beginning (B) and at the end (E) of the stability tests shown in Figure 4 in comparison with the thermodynamic predictions.

Sample	YCO (%)	YCO ₂ (%)	YCH ₄ (%)	YC ₂ H ₄ O (%)	YC ₃ H ₆ O (%)	YC ₂ H ₄ (%)
Powder B	11	61	33	0.01	0.01	0.01
Powder E	22	52	18	0.5	0.7	1.3
Foam B	9	56	34	0.02	0.02	0.01
Foam E	6	61	36	0.02	0.02	0.02
Thermodynamics	9	63	29	-	-	-

The metallic nature of the support, combined with the continuous and thermally connected structure, assures a relevant enhancement of radial heat transfer in reforming reactors loaded with catalytic foams in comparison with traditional packed bed reactors for highly exothermic heterogeneous catalytic processes. Enhanced global heat transfer rates in conductive foams can decrease axial and radial temperature gradients, minimizing hot (or cold) spots (Tronconi et. al. 2014).

After the 24 hours of time-on-stream, the spent catalysts were characterized via TPO measurements (described in Par.2) and it was possible to quantify the extent of deactivation for the two samples. It is very interesting to note that the carbon formation rate recorded over the structured catalyst is very close to the value found in the case of the powder having the same formulation (Table 2). In fact, the foam catalyst specific structure as well as its high thermal conductivity assures to manage almost the same amount of carbon without any apparent activity loss.

4. Conclusions

In this work, oxidative steam reforming of ethanol has been investigated in the presence of a Pt-Ni catalyst supported on CeO₂-Al₂O₃. In particular, the latter formulation was optimized by testing samples prepared with a Pt loading in the interval 2-5 wt% and CeO₂/Al₂O₃ ratio ranging from 25 to 45 wt%. The endurance performance of the catalysts was studied at 500°C under an H₂O/C₂H₅OH ratio of 4 and O₂/C₂H₅OH ratio of 0.5; reaction temperature was fixed to 500°C while the WHSV was equal to 12 h⁻¹. The best results in terms of catalysts durability were achieved by choosing 3 wt% for Pt and 35 wt% for ceria, such formulation assures the best ceria dispersion and the lowest carbon deposition rate. The performance of the most promising powder catalyst was compared with the OESR activity of a foam catalyst prepared starting from the same formulation. A clear improvement in terms of selectivity and stability was recorded: ethanol conversion and hydrogen yield profile

were very stable with time-on-stream in the presence of the structured catalyst and the by-products formation was negligible both at the beginning and at the end of the test (after 24 hours). These results are ascribable to the good thermal properties (high thermal conductivity) and to the enhanced mass transfer coefficient assured by the foam catalyst.

Acknowledgments

The authors wish to thankfully acknowledge Dr. Roberto Clerici (Sasol Performance Chemicals) for providing the alumina used in this work.

References

- Anil S., Indrajya S., Singh R., Appari S., Roy B., 2022, A review on ethanol steam reforming for hydrogen production over Ni/Al₂O₃ and Ni/CeO₂ based catalyst powders, *International Journal of Hydrogen Energy*, 47, 8177, 8213.
- Bilal M.; Jackson S.D., Ethanol steam reforming over Pt/Al₂O₃ and Rh/Al₂O₃ catalysts: The effect of impurities on selectivity and catalyst deactivation, 2017, *Applied Catalysis A: General*, 529, 98-107.
- Cerdá-Moreno C.; Da Costa-Serra J.F.; Chica A. Co and La supported on Zn-Hydrotalcite-derived material as efficient catalyst for ethanol steam reforming, 2019, *International Journal of Hydrogen Energy* 44, 12685-12692.
- Fang B., Qi Z., Liu F., Zhang C., Li C., Ni J., Lin J., Lin B., Jiang L., 2022, Activity enhancement of ceria-supported Co-Mo bimetallic catalysts by tuning reducibility and metal enrichment, *Journal of Catalysis* 406, 231-240.
- Guo W., Li G., Zheng Y., Li K., Guo L., 2022, Influence of La₂O₃ addition on activity and coke formation over Ni/SiO₂ for acetic acid steam reforming, *International Journal of Hydrogen Energy*, 47, 3633-3643.
- Kumar D., Juneja A., Hohenschuh W., Williams J.D., Murthy G.S., 2012, Chemical composition and bioethanol potential of different plant species found in Pacific Northwest conservation buffers, 4, 63114-63124.
- Lazar D.M., Senila L., Dan M., Mihet M., 2019, Crude Bioethanol Reforming Process: The Advantage of a Biosource Exploitation, *Ethanol Science and Engineering*, 10, 257-288.
- Mulewa W., Tahir M., Saidina Amin A.S., 2017, Ethanol Steam Reforming for Renewable Hydrogen Production over La-Modified TiO₂ Catalyst, *Chemical Engineering Transaction*, 56, 349-354.
- Palma V., Ruocco C., Meloni E., Ricca A., Coke-resistant Pt-Ni/CeO₂-SiO₂ Catalysts for Ethanol Reforming, 2017, *Chemical Engineering Transactions*, 57 1675-1680.
- Peres A.P.G., Lunelli B.H., Filho R.M., 2013, Application of Biomass to Hydrogen and Syngas Production, *Chemical Engineering Transactions*, 32, 589-594.
- Ruocco C., Palma V., Cortese M., Martino M., 2022, Stability of bimetallic Ni/CeO₂-SiO₂ catalysts during fuel grade bioethanol reforming in a fluidized bed reactor, *Renewable Energy*, 182, 913-922.
- Ruocco C., Palma V., Ricca A., 2019, Hydrogen production by oxidative reforming of ethanol in a fluidized bed reactor using a Pt-Ni/CeO₂-SiO₂ catalyst, *International Journal of Hydrogen Energy*, 44, 12661-12670.
- Souza E.L., Liebl G.F., Marangoni C., Sellin N., Montagnoli M.S., Souza O., 2014, Bioethanol from Fresh and Dried Banana Plant Pseudostem, *Chemical Engineering Transactions*, 38, 271-276.
- Tronconi E., Groppi G., Visconti C.G., Structured catalysts for non-adiabatic applications, 2014, *Current Opinion in Chemical Engineering*, 5, 55-67.
- Xu T., Wang X., Xiao B., Liu W., 2021, Single-step production of hydrogen-rich syngas from toluene using multifunctional Ni-dolomite catalysts, *Chemical Engineering Journal*, 425, 131522-131532.